

Designing with Gamma Titanium
CAESAR Program
Titanium Aluminide Component Applications

Dwight E. Davidson

Pratt and Whitney Aircraft Engines
Government Engines and Space Propulsion Division
Advanced Engines Programs
West Palm Beach, Florida 33410

Abstract

The United States Government embarked on the Integrated High Performance Turbine Engine Technology (IHPTET) initiative to double the thrust to weight (Fn/Wt) performance from baseline turbine engines produced in the mid 1980's. In order to achieve these improvements, increases in engine systems temperature and pressure and decreases in weight must be simultaneously accomplished. Under IHPTET, the United States Air Force (USAF) funded the Component and Engine Structural Assessment Research (CAESAR) Program, whose goal is to demonstrate the rules and tools of the design intent for transitioning new materials. Of these materials, this article will critically review gamma titanium aluminide (TiAl), and comment on design issues, material property comparisons and manufacturing challenges required for successful static and rotating component demonstration.

Introduction

The CAESAR Program provides for the structural assessment of several key technologies in a multi-company endeavor involving Pratt and Whitney Aircraft (PWA), General Electric Aircraft Engines (GEAE), Rolls Royce Inc US/UK (RR) and Allison Advanced Development Company (AADC). These technologies are to be tested in an Advanced Turbine Engine Gas Generator (ATEGG) core. IHPTET has 3 phases. The CAESAR core will

subject the TiAl blades to IHPTET Phase I environmental conditions. Following this test, the blades will be subjected to a planned structural test for up to 2000 Total Accumulated Cycles (TAC) of durability in an engine environment. The complete test plan will yield durability data at conditions expected for production use, thus providing a base from which to assess various TiAl material systems and correlate new design criteria. The CAESAR Program TiAl technologies are:

- Attached Compressor Blades
- Combustor Fuel Nozzle Swirlers
- Compressor Variable Vane Shrouds
- Engine Nozzle Tiles

This article will critically review TiAl component development pertaining to the High Pressure Compressor (HPC). Areas to be covered are:

- Environmental Requirements
- Material Definition
- Design Considerations
- Lifing Methods
- Manufacturing Challenges

Clearly, the HPC blade, which is a rotating application, required a more rigorous structural analysis than the shroud, a static component. Thus, the HPC blades paved the way in establishing design criteria, manufacturing know-how and pretest validations.

Environmental Requirements

HPC Attached Blade

The HPC Attached Blades are designed to meet the F119 full mission requirements (8600 TAC and 5000 hours of service life). The blades are capable of achieving metal temperatures of 1000°F for up to 1000 hours and 1300°F for up to 10 hours. The CAESAR program engine test, which will subject these blades for up to 2000 TAC, could impose up to 1/4 of the primary life (HCF and Creep) requirement in a short amount of time. After post engine testing, environmental effects (oxidation, material stability, crack growth resistance etc) on the blades will be measured and correlated into existing lifing and design criteria.

HPC Variable Vane Shroud

The Variable Vane Shrouds will also be required to meet the F119 full mission requirement. The CAESAR/F119 engine test could impose a metal temperature of 700°F for up to 1000 hours and 1000°F for up to 10 hours. For this application the primary property of interest is wear. To date, an initial wear coating containing cobalt, chromium and tungsten has passed a 1200°F, 500 cycle thermal shock test. In all variable vane stages the vane stem material is titanium; therefore, for environmental considerations, protecting against titanium to titanium wear is a requirement.

Material Definition

PWA TiAl blades for the CAESAR program were cast by HOWMET Corporation using Ti-47Al-2Mn-2Nb-0.8%TiB₂¹ (47XD) with a duplex microstructure.

To minimize cost and schedule delays typically encountered for a development program, all of the CAESAR component castings were produced from tooling made from 3 dimensional stereo lithographic models. Components were investment cast using the "lost wax" technique and single Vacuum Arc Remelting (VAR) process. In all cases the castings were overstocked between .020-.080 inches and machined into final configuration. All of the castings

were HIP'ed at 2300°F and 25 ksi for 4 hours followed by an 1850°F and 50 hours heat treat.

HOWMET performed tensile and creep qualification test from each heat of material provided for each component. In all cases, tensile and creep data from every component heat met or exceeded design specifications. Table I presents comparative tensile properties of 47XD and wrought IN100.

Table I. Comparative Material Property of 47XD and IN100

	70F	Temp	1200F
47XD			
Tensile Strength (ksi)	71		70
Yield Strength (ksi)	55		47
Elong. (% in 4D)	1.2		2.6
Modulus (lb/in ² E6)	24		21
Density (lb/in ³)		0.143	
IN100			
Tensile Strength (ksi)	220		190
Yield Strength (ksi)	155		155
Elong. (% in 4D)	14		14
Modulus (lb/in ² E6)	31		26
Density (lb/in ³)		0.284	

Design Considerations

All of the TiAl components tested had a specific goal of either; offering better performance, reducing system weight or lowering cost. In the case of the HPC Attached Blade, better performance in the form of temperature capability was of primary benefit. Weight was a secondary benefit, while cost was hard to evaluate, especially under a development program. Since the Variable Vane Shrouds has a near term transition path to the F119 program, cost and weight were the driving factors.

HPC Attached Blade

The F119 development engines use attached nickel blades, which offer a means to swap and upgrade airfoils during testing. Two features on the basic nickel design were modified on the TiAl blades, the airfoil shape and the attachment bearing surface. In both cases the bearing surface area and the airfoil thickness were increased 20% and 40% respectively. In addition, the thicker airfoils reduced the overall flow area between each airfoil. To compensate for this

¹Chemistry is given in atomic percent

reduced flow, slight airfoil chordwise rechambering and spanwise bowing were introduced into the geometry. In essence this was done to minimize performance losses associated with thicker airfoils.

The total HPC blade height, including airfoil, is 1.2 inches. The airfoil height alone is 0.9 inches. while the chord length is 0.7 inches. The airfoil root thickness starts at 0.11 inches and decreases to 0.03 inches at the tip. The airfoils are bowed tangentially against the direction of rotation. The bowed airfoil root intersect the platform of the blade with a -5 degrees incidence angle and ends up with a +18 degree incidence angle at the blade tip. One hundred ten TiAl blades are designed to fit into a nickel based superalloy (IN100) rotor. See Figure 1.

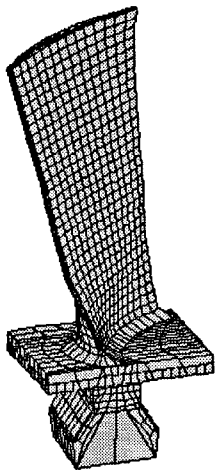


Figure 1. HPC Attached Blade

TiAl blades, with a density half that of nickel based superalloy blades, realized a total of 0.5 pounds of static weight savings. Secondary weight savings, due to rotational effects, could have been realized in the nickel disk, but were reintroduced back into the rotating system to allow for greater creep resistance at higher operating temperatures. In all, the TiAl attached blades weight savings to the CAESAR program were minimal; however, the temperature capabilities of the airfoils were increased several hundred degrees. (See section on Lifting Methods)

HPC Variable Vane Shroud

The F119 Engineering, Manufacturing, and Development (EMD) engines use a ceramic matrix composite (CMC) as its Variable Vane Shroud bill of material. Because of the CMC high production cost, associated with consolidating plies of glass and epoxy

fibers, and its low overall industry production requirement, a less costly replacement was required.

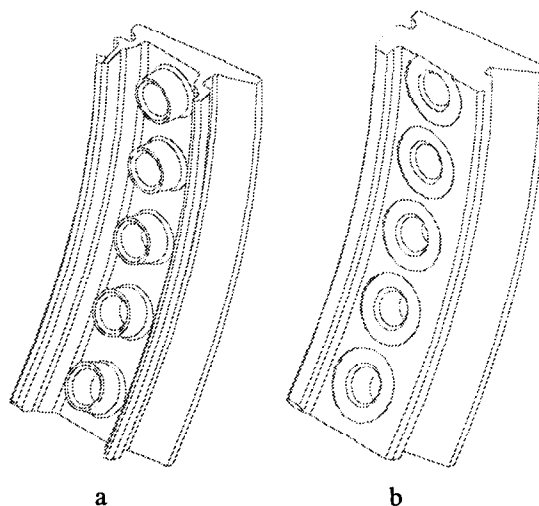


Figure 2. Design Comparison of HPC Variable Vane Shroud Fabricated from a) TiAl b) CMC

The HPC Variable Vane Shrouds are cast as segments with a 36 degree included arc. Ten pieces are required per assembly. Total radial thickness is 0.75 inches while the total axial length is 2.0 inches. Allowed minimum wall thickness after machining is 0.10 inches. At assembly the variable vane stems are fitted though each shroud hole and bolted together from the under side. No threaded features are machined into the TiAl hardware.

Table II Comparative Geometric Properties of 47XD versus CMC Shroud

TiAl Shroud		CMC Shroud
0.143	Density (lb/in ³)	.087
2.24	Segment Volume (in ³)	4.07
0.32	Segment Weight (lb)	0.35
3.32	Stage Weight (lb)	3.64

Since the CMC shroud application and its location, would not push the material to its temperature envelope, would not allow for the weight increases by going to a nickel alloy, and were too hot for the use of conventional titanium, TiAl castings were the logical candidate. TiAl cast shrouds offered multiple material sources, multiple material types (alloy and microstructure), more ductility, higher strength and higher strain to failure than CMC for this application. With its higher density than CMC a TiAl based shroud had to do a better job achieving its weight goals. This was done by hollowing out pockets

of material in noncritical areas of the component. See Table 2 and Figure 2a and Figure 2b.

The hollowed out design of the HPC Variable Vane Shroud required no further rigorous analysis. The other critical design feature to consider was its wear characteristics. TiAl shrouds with a coating, would be competing with CMC shrouds that do not require a wear coating at all.

Lifing Methods

For most component design, a rigorous structural analysis is required to ensure that they would survive testing and that they would meet full life. The classic types of design information that are required to perform such an analysis are creep data, low cycle fatigue data, high cycle fatigue data and fatigue crack growth data. The basis and ultimately the criteria for these types of components can be derived from specimen testing.

HPC Attached Blade

Figure 3 was derived from fatigue crack growth specimen test data. Standard compact tension specimen were used to generate a da/dN versus ΔK data set. From the da/dN versus ΔK data, Stress versus Cycles (S-N) curves were produced for various combinations of crack size, crack shape, R-ratio and temperature.

Figure 3 compares the elastic stress versus cycles for a surface flaw size of .015 inch, R-ratio = 0.1 at a temperature of 1200°F of IN100 to that of a 47XD alloy. IN100 strengths range from 160 ksi @ 1000 cycle (typically associated with K_{IC} on a da/dN versus ΔK curve) capability, to 80 ksi @ 9000 cycle (typically associated with ΔK_{th} on a da/dN versus ΔK curve) capability. TiAl strengths range from 70 ksi @ 1000 cycles capability to 45 ksi @ 100,000 cycle capability. Regardless of temperature, R ratio, crack size or crack type, all other combinations of fatigue crack growth S-N curves yielded the same type of results.

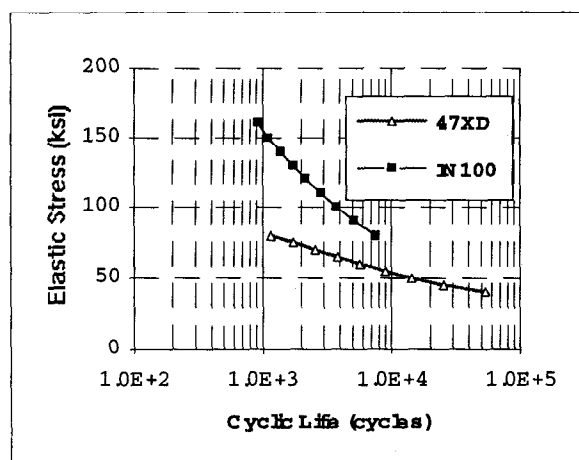


Figure 3 Elastic Stress versus Cycles
Surface Flaw Model with 0.015 Initial Crack Size
at 1200°F, R Ratio = 0.1

At first glance, IN100 appears superior to 47XD. If however, the results in Figure 3 are analyzed more closely by normalizing for the density difference, the results would allow a design engineer to compare more accurately material systems to each other for rotating or static applications.

Figure 4 compares the density normalized elastic stress versus cycles for a surface flaw size of .015 inch, R-ratio = 0.1 and a temperature of 1200°F for 47XD and a IN100. Across all stress levels and cycles, 47XD is as good as if not better than the IN100 in a rotating application (density normalized).

The data presented in Figure 4 were tested from the HOWMET 47XD material system which has a duplex microstructure. It has been reported in recent literature [ref 1,3,4] that a lamellar based microstructure has a higher ΔK_{th} than a duplex based material system. Therefore one could speculate that improvements in the existing data presented in Figure 4 are possible.

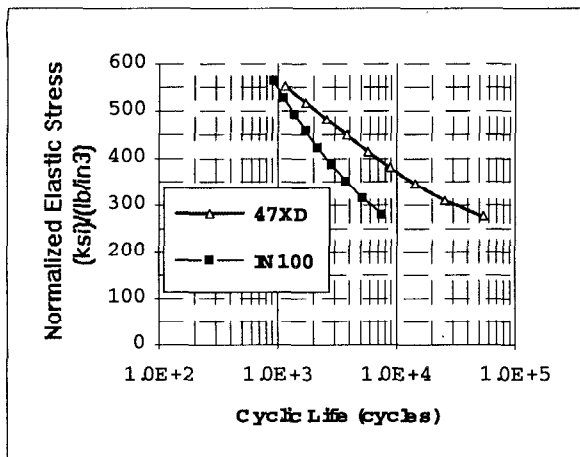


Figure 4 Density Normalized Elastic Stress versus Cycles
Surface Flaw Model with 0.015 Initial Crack Size
at 1200°F, R Ratio = 0.1

Another criteria that is used in designing hardware that operates in high vibratory environments, is a Modified Goodman Diagram. Figure 5 was derived from smooth cylindrical High Cycle Fatigue (HCF) test specimen data. These specimens were tested at R-ratios of -1.0, 0.1, and 0.5 and over a range of temperatures between 70°F to 1400°F.

Figure 5 compares the allowable elastic vibratory stress of a IN100 to that of 47XD. IN100 strengths for an R-ratio = -1.0 (endurance limit stress @ $10E^7$ cycles; i.e., fully reversed bending) at temperature of 1200°F is 125 ksi. The endurance strength limit of 47XD is 85 ksi. In addition, the IN100 steady stress allowable and the TiAl steady stress allowables are 210 ksi and 60 ksi respectively. A line drawn between these points determines a high cycle fatigue endurance limit for a range of steady stress and vibratory stress. Again, IN100 looks better than 47XD in HCF capability.

If the results in Figure 5 are analyzed more rigorously by normalizing the elastic allowable steady stress of the material. This would yield a normalized specific steady stress allowable. These results would allow a design engineer to compare any material systems in HCF for rotating application.

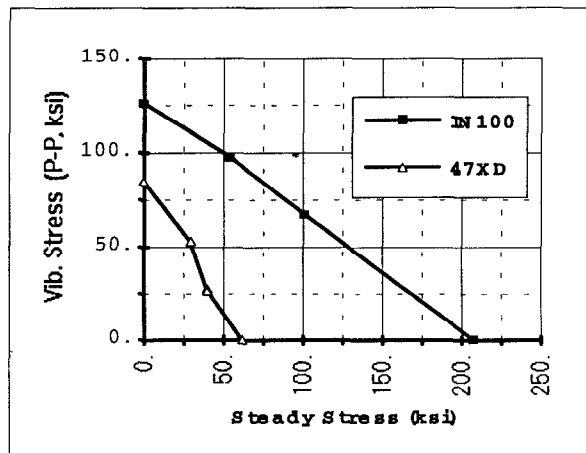


Figure 5. Modified Goodman Diagram Comparing IN100 to 47XD at $10E^7$ cycles and 1200°F

Figure 6 is a plot of allowable elastic vibratory stress versus normalized specific steady stress for 47XD and IN100. In this case, cast 47XD material properties are not quite as good as the IN100 material. The graph presented was taken from a sample of 1200°F test data. As temperature continues to increase to 1400°F the IN100 fatigue capability decays rapidly towards zero. As temperature continues to increase towards 1400°F the 47XD fatigue properties remain constant and in fact increase slightly. For cast properties 47XD is not quite as good as IN100 up through 1200°F. Above 1250-1300°F it then become desirable to switch to TiAl because of the intrinsic density benefits.

A secondary benefit for using TiAl can be derived from other literature [ref 9,10]. Typical alloys exhibit HCF and LCF endurance behavior that track closely with the yield strength of the material. Wrought TiAl when processed via extrusion and/or forgings has reported yield strengths of 100 ksi or higher at room temperature. If these data points are incorporated into the existing Modified Goodman Diagrams one could estimate that wrought TiAl is as good as if not better than IN100 across all temperature ranges and stress levels for rotating applications.

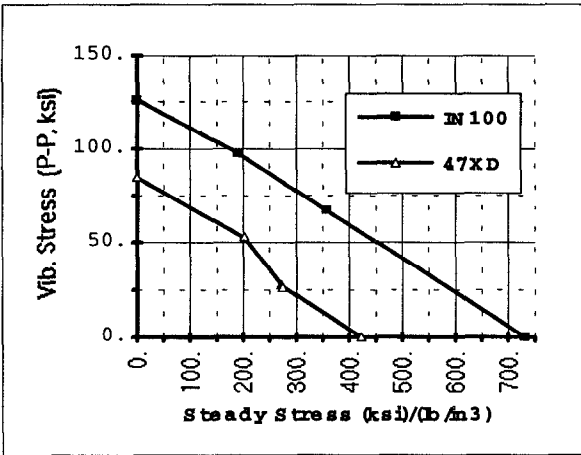


Figure 6. Modified Goodman Diagram
Vibratory Stress versus Density Normalized
Steady Stress at 1200°F and 10E⁷ cycles

Another criteria that is used to design hardware that operates in severe cyclic environments, is Low Cycle Fatigue (LCF). Figure 7 was derived from smooth cylindrical LCF test specimen data. These specimens were tested at R-ratios of 0.1, and 0.5 and over a range of temperatures from 70°F to 1400°F.

Figure 7 compares the allowable elastic stress versus cycles of IN100 to that of 47XD. IN100 cyclic capability to crack initiation for an R-ratio of 0.1 is 175 ksi @ 1000 cycles and 1200°F. 47XD cyclic capability to crack initiation for an R-ratio of 0.1 is 55 ksi @ 1000 cycles and 1200°F. In addition IN100 based LCF endurance limit @ 10E5 cycles is 80 ksi. Gamma titanium endurance limit @ 10E5 cycles is 50 ksi. A line drawn between these points determines the remaining cycles and stress levels required for crack initiation. As in prior figures IN100 looks superior to 47XD.

It is truly in LCF resistance where the commercial utilization of nickel based superalloys has won out in the last 30 year. This curve is indicative of the ability of nickel based superalloys to be able to tolerate hammer blows, dings, abusive handling, etc without the worry of premature failure.

If we density normalize the LCF data as was done with the crack growth and HCF normalized data, little improvement in TiAl LCF properties are realized. See Figure 8.

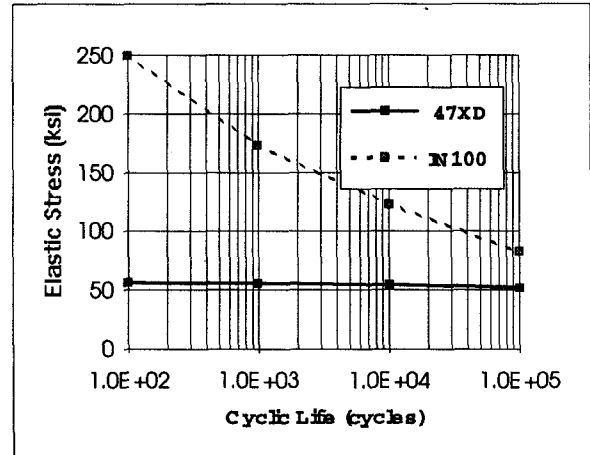


Figure 7. Low Cycle Fatigue Elastic Allowable
Stress versus Cycles at 1200°F

Figure 8, however, does offer some additional insight [ref 9,10]. Typically, alloys exhibit HCF and LCF endurance behavior that track closely with the yield strength of the material. Wrought TiAl, when processed via extrusion and/or forgings has reported yield strengths of 100 ksi or higher at room temperature. If these data are incorporated into the LCF design data base, one could estimate that TiAl LCF capability would be as good as if not better than nickel based superalloys across all temperature ranges where endurance (> 1E⁴ cycles) becomes a driving product requirement. Such applications would be industrial gas turbines, long range unmanned reconnaissance aircraft, aircraft auxiliary power unit, etc.

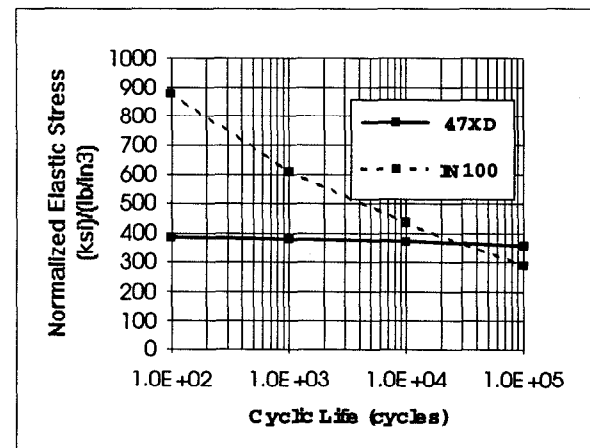


Figure 8. Low Cycle Fatigue Density Normalized
Elastic Allowable Stress versus Cycle at 1200°F

This leads us to the last important design criteria, which helps designers make application decisions, creep based life behavior. Figure 9, a Larson-Miller plot, was derived from smooth round and smooth flat tensile creep specimen. These specimens were tested over a range of temperatures from 70°F to 1400 °F.

Figure 9 compares the allowable creep stress of IN100 to that of 47XD. IN100 0.2%/10hr/1200°F creep capability is 125 ksi. 47XD 0.2%/10hr/1200°F creep capability is 45 ksi. In addition IN100 0.2%/1000hr/1200°F creep capability is 100 ksi. 47XD 0.2%/1000hr/1200°F creep capability is 30 ksi. A curve drawn between these points determines an overall stress allowable versus time for material usage at temperature. As in the prior graphs IN100 appears better than 47XD.

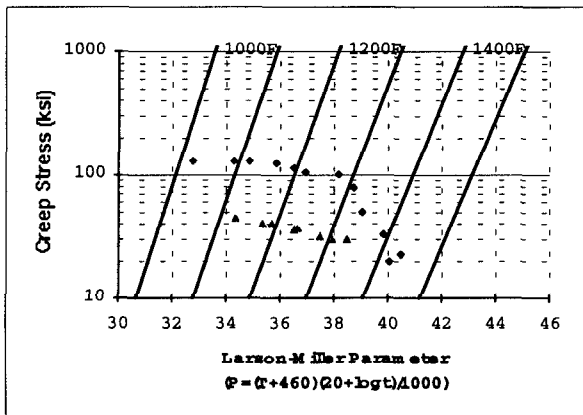


Figure 9 0.2% Larson Miller Creep Parameter
 Δ = TiAl \diamond = IN100

Density normalization reveals a much clearer picture. Figure 10 shows that TiAl has comparable normalized stress levels to that of IN100 at 1300°F and above and near comparable stress levels as IN100 at lower temperatures.

A secondary benefit of TiAl can be derived from other literature [ref 5-8] on its creep response. Most alloys exhibit improvements in creep capability when the material is hot worked during consolidation. Wrought TiAl, when processed via extrusion and/or forging have reported creep capabilities several hundred degrees beyond the 47XD creep capabilities shown in Figure 10. Thus, it can be anticipated that substantial increases in creep strength will be

achieved in TiAl alloys through chemical modifications and microstructural control.

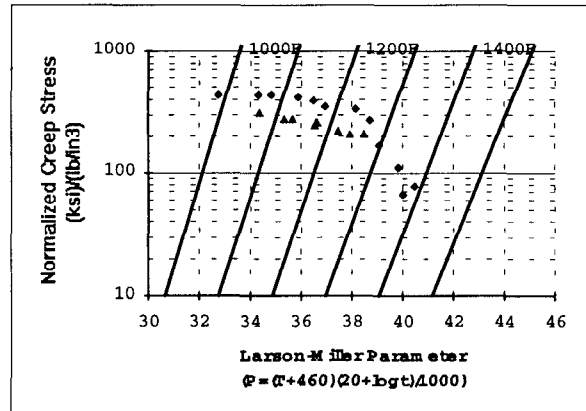


Figure 10. Density Normalized
 Larson Miller Creep Parameter
 Δ = TiAl \diamond = IN100

Manufacturing

HPC Attached Blade

The four participants in the CAESAR Program, GEAE, PW, RR, AADC, each used its own TiAl material system and manufacturing methodologies. GEAE and AADC provided their blades in wrought form, while PW and RR provided their blades in cast form.

Specifically, AADC electro-chemically etched (ECM'ed) its airfoils and ground its dovetails. RR EDM'ed its entire blade, while both PW and GEAE milled their airfoils and grounds their dovetails. An unusual item was that each of the four contractors used widely different final stress relief schedules.

Elaborating on PW manufacturing details, PW used conventional carbide milling tools with conventional speeds and feeds. The dovetails were ground using diamond tools with very fine grit sizes. For comparison, United Technology Research Center (UTRC), determined a machinability rating for 47XD that lies somewhere between IN100 and conventional titanium alloys.

All of the CAESAR participants have agreed to perform cleaning tests for TiAl. Concerns that have been raised are:

- a) can TiAl tolerate multiple acid/alkali cleaning, without forming cracks, over the service life of the parts
- b) does TiAl pick up surface hydrogen, which can help form cracks during machining, thus making the parts unusable.

HPC Variable Vane Shroud

As highlighted in "Design Considerations", for the shrouds, cost was the primary driver; specifically, the raw material cost of the CMC shroud. Switching to cast TiAl shrouds produced an overall cost benefit.

The secondary cost benefit for TiAl shrouds came from manufacturing. As illustrated in Figure 11a and Figure 11b, the CMC based shroud had to have every surface feature machined. By contrast the TiAl cast shroud only has the critical features machined (contact areas, through holes and outside diameters). The rest of the part remains in the as-cast state. This reduces the number of setups, the number of tools and time on the machining centers.

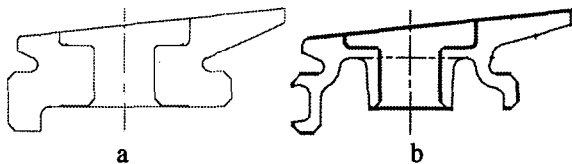


Figure 11. Manufacturing Comparison of HPC Variable Vane Shroud Fabricated from
a) CMC b) TiAl

The one cost detriment for cast TiAl shrouds, was the cost of a wear resistant coating for the holes. The overall cost summary however still yielded a favorable cost analysis for switching to TiAl shrouds.

Finally, the commercialization of TiAl (blade or shrouds, static or rotating) will be driven by Life Cycle Cost benefits gained through either weight reductions or value analysis. Near term cost of cast TiAl ingots, casting tooling and machining will keep the cost higher than conventional titanium and conventional nickel hardware, until scale up of wrought TiAl to full sizes can be achieved repetitively.

Conclusions and Observations

Extensive progress and improvements in titanium aluminides have been made in the last decade. Industry has progressed from first generation cast alloys with moderate strength, poor ductility and process control problems, to second generation alloys in both cast and wrought form that have better overall properties and better process control. These second generation alloys have yielded multiple hardware demonstrations most notably at General Electric but also at Pratt and Whitney, Rolls Royce and many of the other gas turbine engine manufacturers in the United States and abroad.

Based on the comparative material properties, TiAl has superior fatigue crack growth and creep resistance over IN100. As shown, improvements in both weight and performance can be achieved in rotating applications. TiAl, with its limited ductility and LCF capabilities compared to IN100 will see little weight advantage in most static applications, but should see modest end use in hot static applications where impact and foreign object damage are not of great concern. Regardless of application, TiAl's broader use in the commercial world (manned use) will still be limited until issues concerning validation of design system and durability, low toughness, limited ductility and low threshold stress levels are fully understood.

As far as unmanned applications, TiAl offers an improved risk picture. With material properties comparable to nickel based alloys, TiAl should see quick and continued expansion in unmanned design applications, especially for rotating and static hardware where long endurance is envisioned. Industrial gas turbine products, long endurance Unmanned Aerial Vehicles (UAV), IHPTET and Advanced Concept propulsion systems that have repetitive long mission requirements are prime examples. Only after gaining experience and correlating design systems will TiAl be introduced for broad "manned" applications.

All CAESAR TiAl hardware applications were processed from existing foundry and machining centers. No new capital equipment was required to produce these parts. It is therefore envisioned that the expanded use of this alloy will rely heavily on industrial scale up. Industry will have to learn to deal

with producing full size cast ingots and learn innovative foundry techniques to increase yields for cast and wrought hardware.

Acknowledgments

The author would like to acknowledge the research and development activities of his colleagues D. R. Clemens, C. I. Lobo at Pratt and Whitney, Dr. D.L. Anton from United Technology Research Center, D.E Thomson and M.F. Huffman from USAF Wright Labs, Structures Branch, from which these discussions have been based.

References

Published Papers

1. Venkataswara Rao, K.T., Y. W. Kim , R.O. Ritchie, Fatigue Crack Growth and Fracture Resistance of Two Phase TiAl Alloy in Duplex and Lamellar Microstructure, *Scripta Metallurgica et Material*, 1995.
 2. T. G. Nieh, J.N. Wang, Stress Change and its Implication for the Reduction of Primary Creep in Gamma TiAl, *Scripta Metallurgica et Material*, 1995.
 3. J.M. Larsen, B.D. Worth, S.J. Balsone, A.H. Rosenberger, J.W. Jone, Mechanism and Mechanics of Fatigue Crack Initiation and Growth in TiAl Intermetallic Alloys, *Fatigue* 1996.
 4. J.M. Larsen, B.D. Wörth, S.J. Balsone, J.W. Jone, An Overview of the Structural Capability of Available Gamma Titanium Alloys, TMS World Conference 1995.
- ##### Unpublished Papers
5. T.G.Nieh, et al Development of Micro-Toughened Gamma TiAl and its Composites LLNL 1996.
 6. C.T Lui, et al Development of Micro-Toughened Gamma TiAl for High Temperature Service ORNL 1996.
 7. V.K Sikka, et al Processing of TiAl Intermetallics Alloys and Micro-Toughened Composite ORNL 1996.
 8. P.J. Maziasz, et al Microstructural Analysis of Gamma TiAl Alloys Base on Ti-47Al-2Cr-2Nb, ORNL 1996.
 9. D.R. Clemens, R.A. Anderson, Creep and LCF/HCF Behavior of TiAl Material for NASP, PW 1990.
 10. D.R. Clemens, C.I.Lobo, Creep and HCF/LCF Behavior of TiAl Material for CAESAR, PW 1993.
 11. P.L. Martin, Creep and Process Control of TiAl Material for MSF, RRSC 1995-1996.